ELSEVIER

Journal of Alloys and Compounds 323–324 (2001) 623–627

Journal of ALLOYS AND COMPOUNDS

www.elsevier.com/locate/jallcom

De Haas-van Alphen effect in $LuAl_3$

I. Sakamoto[a,*], G.F. Chen[a], S. Ohara[a], H. Harima[b], S. Maruno[a]

[a]*Department of Electrical and Computer Engineering, Nagoya Institute of Technology, Showa-ku, Nagoya 466-8555, Japan*
[b]*Department of Condensed Matter Physics, The Institute of Scientific and Industrial Research, Osaka University, Osaka 567-0047, Japan*

Abstract

We have measured the de Haas-van Alphen (dHvA) effect in $LuAl_3$ at temperatures between 1.3 K and 4.2 K in magnetic fields up to 13 T. Observed frequencies range from 400 T to 23 kT. The highest one corresponds to a cyclotron orbit with an area equal to a square face of the Brillouin zone. The angular dependence of the frequencies suggests that the Fermi surfaces are composed of a nearly spherical closed sheet and multiple connected open sheet. The observed cyclotron effective masses for the closed Fermi surface are about 0.7 and those for open Fermi surface range from 0.3 to 1 in units of the free electron mass. A band structure calculation was carried out by a full potential linearized APW method. The gross feature of the observed results was explained by the calculation.

Keywords: $LuAl_3$; de Haas-van Alphen effect; Electronic band structure; Fermi surface; FLAPW method

1. Introduction

The heavy rare earth trialuminide compounds, RAl_3 (where R=Er, Tm, Yb, Lu), crystallize in the cubic $AuCu_3$ type structure. The lattice constants a of RAl_3 [1] decrease gradually from $a=0.422$ nm for R=Er to $a=0.419$ nm for R=Lu, hence rare earth elements in RAl_3 have been considered to be in trivalent state. Among them much attention has been paid to $YbAl_3$, because $YbAl_3$ exhibits valence fluctuation phenomenon, arising from the fact that the 4f levels of $YbAl_3$ are very close to the Fermi level [2–5]. On the other hand, 4f-states in $LuAl_3$ are completely filled and located below the Fermi level. Thus the hybridization of 4f-electrons with conduction electrons is expected to be too small to affect electronic properties in $LuAl_3$. For this reason we have used $LuAl_3$ as a reference material to extract magnetic and electronic properties of $YbAl_3$ caused by 4f-electrons [6]. However, little is known about an electronic band structure and a Fermi surface model for $LuAl_3$ until now. One needs correct knowledge of them to account for electrical properties of $LuAl_3$.

The aim of this work is to investigate the Fermi surface properties and energy band structure of $LuAl_3$ by the dHvA effect. The dHvA effect is one of the most useful tools for these purposes because it allows us not only determine the shape of the Fermi surface but also to determine quasi-particle properties of electron such as electron effective mass and electron lifetime. We also aimed to calculate an electronic band structure of $LuAl_3$ and to present figures of the calculated Fermi surface. The calculated results are compared with the experimental ones.

2. Experimental

Single crystals of $LuAl_3$ were grown from metallic flux [7]. The purity was 4 N for Lu and 6 N for Al. The starting material of Lu:Al in an atomic ratio 4:96 was put into an alumina crucible. The crucible was sealed into a quartz ampoule under high vacuum. The ampoule was heated to 790°C and cooled gradually to 650°C for 2–4 days. The crystals obtained this way had the shapes of cubes, plates and butterfly twins [8] with an angle of 40° between the two wings. The size of each crystal was 0.5–2 mm. The crystals showed the residual resistivity ratios of 20–30. The crystal structure of $LuAl_3$ was checked by an X-ray powder diffraction method with Cu Kα radiation. The lattice constant was determined as 0.4184 nm. This value was used in the present electronic band structure calculation of $LuAl_3$.

The measurements of dHvA effects were performed in a ^{3}He or ^{4}He bath cryostat, which is equipped with a superconducting magnet allowing fields up to 13 T at

*Corresponding author. Tel.: +81-52-735-5151; fax: +81-52-735-5158.

E-mail address: sakamoto@ks.kyy.nitech.ac.jp (I. Sakamoto).

0925-8388/01/$ – see front matter
PII: S0925-8388(01)01193-8

temperatures between 0.35 K and 4.2 K. The crystal was oriented in situ by means of a rotation device. In this manner, measurements were done for magnetic fields in the (100) and (1$\bar{1}$0) zones. A field modulation technique was used to detect the dHvA signal from the pick-up coil. The modulation field amplitude was about 2 mT and its frequency was set at 87 Hz.

3. Results and discussion

Fig. 1(a) shows a typical recorder trace of the dHvA oscillations in the magnetic fields **B** from 7.45 T to 7.75 T parallel to the [110] direction. Fig. 1(b) is the FFT spectrum corresponding to these oscillations. The spectrum contains four fundamental frequencies denoted by α, δ_1, δ_2 and γ. The remaining peaks distinguished by, for example, $\alpha+\gamma$ were identified as combinations of the fundamental frequencies.

Fig. 2 shows an angular dependence of the dHvA frequencies in the (100) and (1$\bar{1}$0) zones. The small filled circles in Fig. 2 are for calculated results we discuss later. The highest frequency (23 kT) observed around the [111] direction corresponds to a cyclotron orbit with an area nearly equal to a square face of the Brillouin zone. The dHvA oscillations for the α branch have shown larger amplitudes for all field orientations. Since the frequencies of the α branch are independent of the field directions, the Fermi surface of the α branch is expected to be nearly a sphere and to be centered on a high symmetry point of the Brillouin zone. The Fermi surface volume for the α branch is estimated to be 23% of the Brillouin zone. The β branch, having moderately large dHvA amplitudes, also shows less field orientation dependence, although it appears only within about 20° from the [100] direction in the (100), (110) zones. The γ branch is seen for all field orientations except around the [001] and [111] directions. The δ_1 and δ_2 branches that appear around the [110] direction have small FFT amplitudes, as shown in Fig. 1(b). Other branches seen in narrow regions of the field directions possessed also very small FFT amplitudes. All observed branch diagrams shown in Fig. 2 indicate that there are at least two Fermi surfaces; one is a closed surface corresponding to the α branch and the other is a multiple connected open surface.

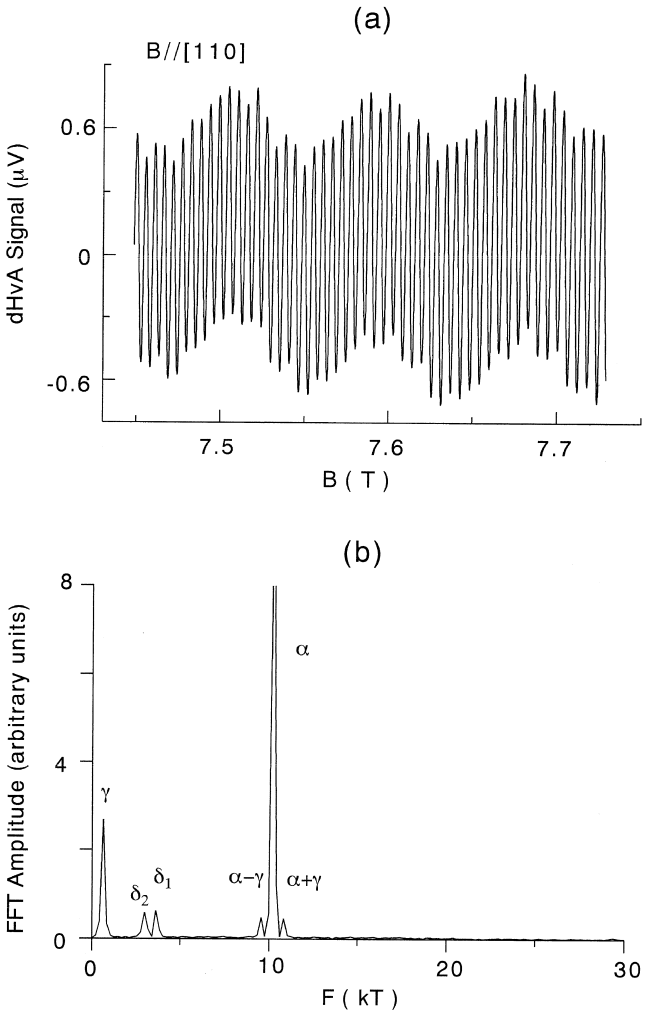

Fig. 1. (a) Typical dHvA oscillations for the [110] direction. (b) FFT spectrum of the oscillations.

We determined the cyclotron masses m_c^* from the temperature dependence of FFT amplitudes between 1.4 K to 3 K in the three principal directions of the crystal. The results are listed in Table 1. The bars in Table 1 indicate that reliable values are not found in the present experiment. The m_c^* values are plotted as a function of the dHvA frequency in Fig. 3. We also plot the values of m_c^* of LuB_{12} measured by Heinecke et al. [9] for comparison. The observed m_c^*/m_0 values for $LuAl_3$ range from 0.3 to 1. This indicates that $LuAl_3$ is one of the normal metals. This is the case for LuB_{12} because the cyclotron masses for $LuAl_3$ and LuB_{12} are in the same range.

To construct a Fermi surface model which is subjected to a rigorous comparison with the experimental results for $LuAl_3$, we have made an improved band structure calculation. The calculation is carried out using a Full potential Linearized Augmented Plane Wave (FLAPW) method with the local density approximation (LDA) for the exchange correlation potential. For the LDA, the formula proposed by Gunnarsson and Lundqvist [10] is used. For the band structure calculation, we used the program codes: TSPACE [11] and KANSAI-99[1]. The scalar relativistic effects are taken into account for all electrons and the spin–orbit interactions are included self-consistently for all valence electrons as in a second variational procedure. The $LuAl_3$ crystal has the space group of $Pm\bar{3}m$. The lattice constant used for the calculation is $a=0.4184$ nm. Muffin-tin (MT)

[1]Program codes for FLAPW calculations have been developed in Japan. One of them is called KANSAI-99, which has been modified and developed in the Kansai area to include the spin–orbit interactions.

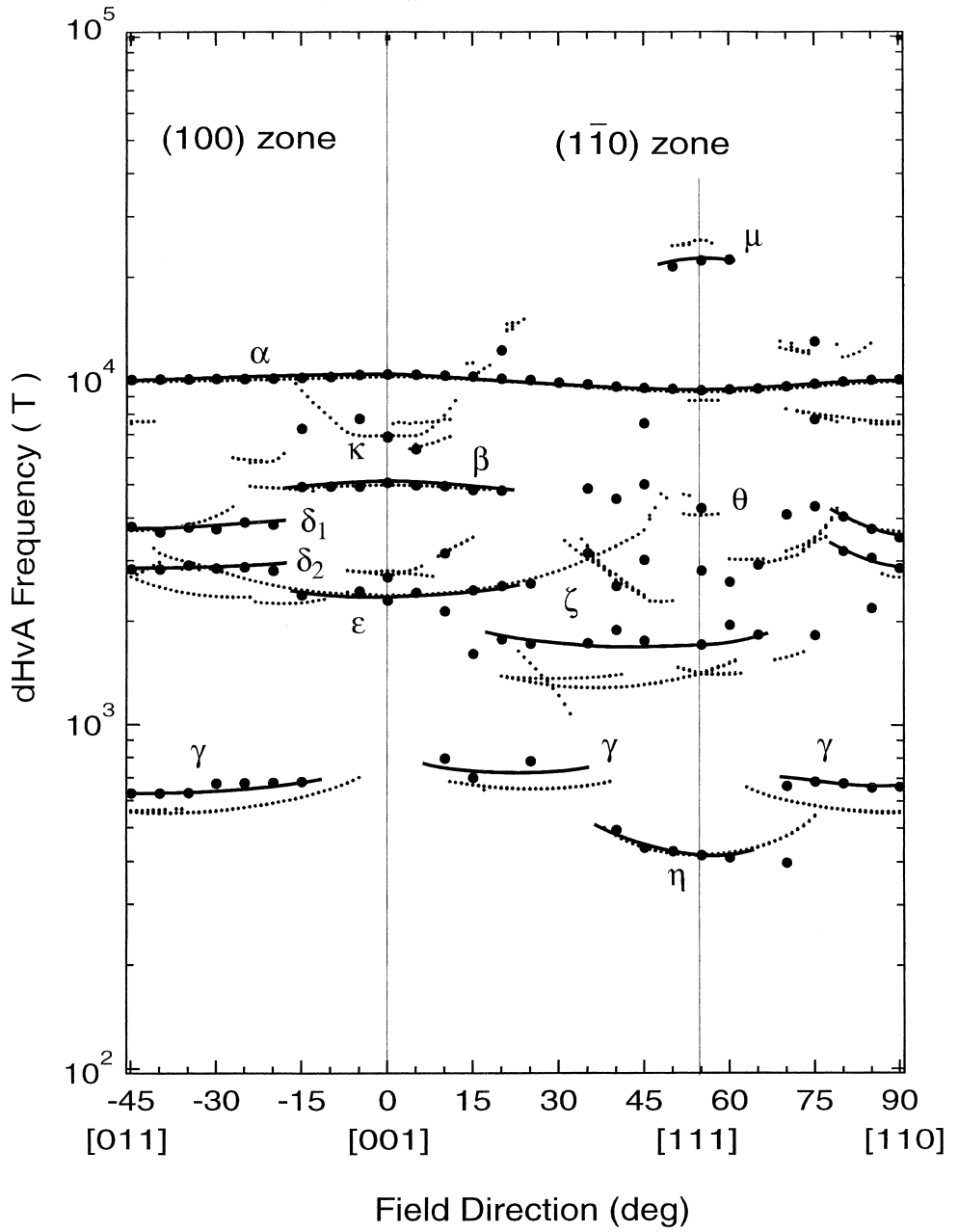

Fig. 2. Variation of the dHvA frequencies with directions of the magnetic field for $LuAl_3$. The calculated frequencies are depicted by the small filled circles. The gross feature of the experimental results is explained well by the calculation.

radii of Lu and Al are set as the same value of 0.33588*a*, because Lu and Al ions are the nearest neighbors in $LuAl_3$. Core electrons (Xe-core minus $5p^6$ for Lu, Ne-core for Al) are calculated inside the MT spheres in each self-consistent step. $5p^6$ electrons of Lu are calculated as valence electrons by using the second energy window. The FLAPW basis functions are truncated at $|\mathbf{k}+\mathbf{G}_i|<4.60\times 2\pi/a$ corresponding to 437 LAPW functions at the Γ point. The sampling points are 286 **k**-points, uniformly distributed in the irreducible 1/48 of the Brillouin zone, both for the potential convergence and the final band structure. Details of the calculation will be published elsewhere.

Fig. 4 shows the calculated band structure. The Fermi level is indicated by E_F. The 4f levels, split by a spin–orbit interaction are located below E_F by 0.31 Ry and 0.42 Ry. The 16th and 17th bands make the Fermi surfaces. The calculated Fermi surfaces are shown in Fig. 5. The hole surface shown in Fig. 5(a) is similar to multiple connected arms along the six equivalent ΓX directions, like a jungle gym, in the reciprocal space and it has an empty region at the symmetry center Γ. The electron surface shown in Fig. 5(b) is spherical but elongated along the ΓX directions. The dHvA frequencies calculated from these Fermi surfaces are shown in Fig. 2 as the small filled circles. The

Table 1
The dHvA frequencies F and cyclotron masses m_c^*/m_o in the three principal directions in $LuAl_3$

Branch	Experiment		Calculation	
	F (kT)	m_c^*/m_0 [a]	F (kT)	m_c^*/m_0 [a]
B//[001]				
α	10.52	0.68	10.30	0.52
	6.92	–	6.94	2.01
β	5.00	0.74	5.00	0.57
			2.80	1.15
	2.71	–	2.73	1.20
ε	2.26	–	2.38	0.45
			2.38	0.86
B//[110]				
α	10.19	0.60	9.98	0.48
			7.64	1.46
δ_1	3.62	0.85	3.68	0.63
δ_2	2.96	0.81	2.69	1.07
γ	0.66	0.3	0.56	0.28
B//[111]				
μ	22.6	–	25.6	2.61
α	9.50	0.60	9.32	0.47
			8.80	1.59
θ	4.27	0.73	4.09	0.55
ζ	1.97	–	1.42	0.69
η	0.48	0.53	0.42	0.20

[a] m_0 is the free electron mass.

electron surface of the 17th band is expected to give only a single branch similar to the branch α. On the other hand, the hole surface of the 16th band gives rise to a variety of branches because of its complicated geometry owing to the multiple connected feature of the Fermi surface.

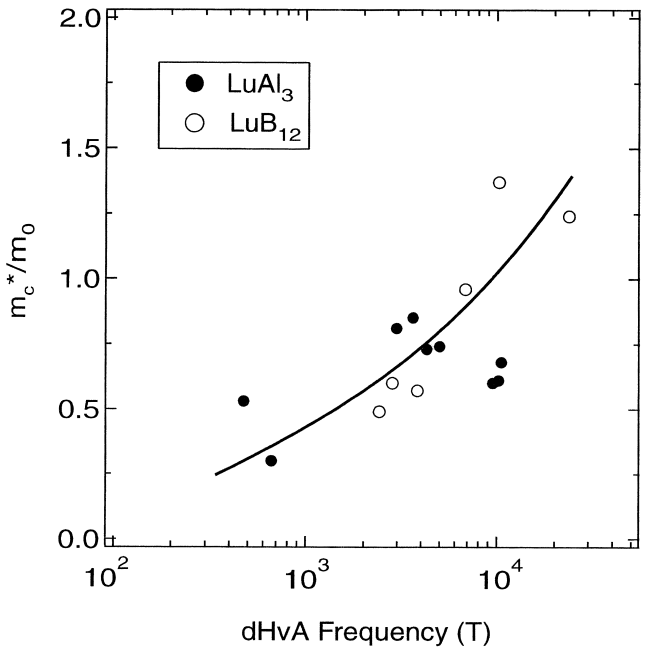

Fig. 3. Cyclotron mass m_c^* in units of the free electron mass m_0 for $LuAl_3$ and LuB_{12} as a function of dHvA frequency. The cyclotron masses for these two materials are in the same range.

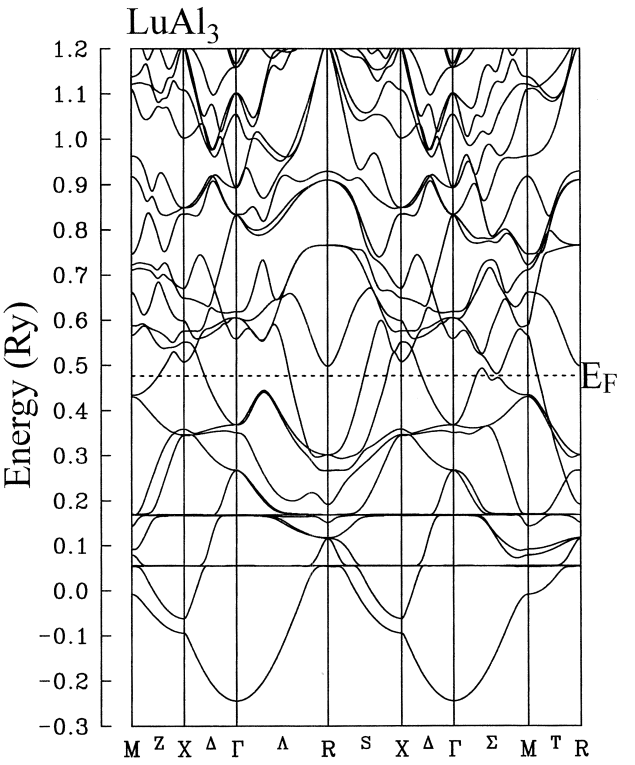

Fig. 4. Energy band structure along the symmetry lines. The Fermi level is denoted by E_F.

Fig. 2 shows that the calculated frequencies for the α branch agree well with the experimental ones both in qualitative and quantitative views. An example of a cyclotron orbit for the α branch is depicted in Fig. 5(b). The branches β, γ, δ_1, ε, η and μ are also well reproduced by the calculation. Some orbits for these branches are also depicted in Fig. 5(a). Although discrepancies between the experiments and calculations are found in the δ_2 and ζ branches, the gross feature of the experimental results is well understood by the calculation.

The cyclotron masses of $LuAl_3$ are also calculated and listed in Table 1 along with the experimental values. The observed m_c^* values are about 1.5 to 2 times larger than the calculated values. This difference is ascribed to the mass enhancement owing to electron interaction that is disregarded in the calculation. Since the cyclotron mass values are the same order of those for normal metals, this enhancement is found to be due to electron–phonon interaction. We note from Table 1 that the present experiment has not detected some dHvA frequencies and the calculated m_c^* values for these frequencies are relatively large. It is known that the dHvA amplitude becomes small as cyclotron mass increases. This is the main reason why we have failed to detect these frequencies.

We can see from Figs. 5(a) and (b) that the Fermi surfaces of the 16th and 17th bands show distinct geometrical characteristics; the local curvatures on the 17th Fermi surface are nearly constant and those on the 16th

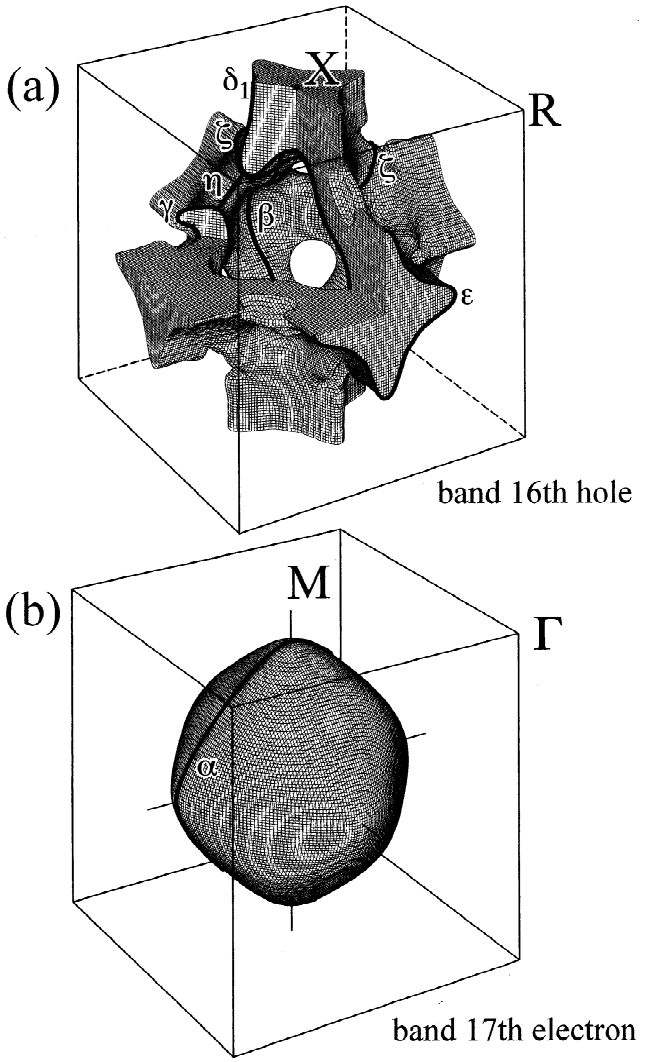

Fig. 5. (a) The 16th band hole Fermi surface centered at the Γ point and (b) the 17th band electron Fermi surface centered at the R point.

band Fermi surface vary remarkably over the Fermi surface. Lifetime of electrons on that part of the Fermi surface where the local curvature is noticeably large is expected to be reduced by electron scattering. Therefore we can speculate that the variation of the electron lifetimes over Fermi surface is more appreciable in band 16th Fermi surface than in the band 17th Fermi surface. This speculation will be examined by measuring the lifetime in the near future.

4. Conclusion

We have measured the dHvA effect for $LuAl_3$. Observed dHvA frequencies ranged from 400 T to 23 kT. The angular dependence of the frequencies showed that the Fermi surfaces are composed of a nearly spherical closed sheet and a multiple connected open sheet. The observed cyclotron effective masses ranged 0.3 m_0 to 1 m_0. We have calculated the band structure for $LuAl_3$ by a FLAPW method. The calculated results explained well the gross feature of the angular dependence of dHvA frequencies. The cyclotron masses were found to be enhanced by a factor of 1.5–2 by electron–phonon interaction.

Acknowledgements

The authors thank Mr. Y. Shomi for technical support. This work was partly supported by a grant-in-aid for Scientific Research from the Ministry of Education, Science and Culture of Japan.

References

[1] P. Villars, Pearson's Handbook of Crystallographic Data For Intermetallic Phases, ASM International, Materials Park, 1997.
[2] U. Walter, E. Holland-Moritz, Z. Fisk, Phys. Rev. B43 (1991) 320.
[3] A. Hiess, J.X. Boucherle, F. Givord, P.C. Canfield, J. Alloys Comp. 224 (1995) 33.
[4] J.J. Joyce, A.J. Arko, A.B. Andrews, R.I.R. Blyth, R.J. Bartlett, J.D. Thompson, Z. Fisk, P.S. Riseborough, P.C. Canfield, C.G. Olson, P.J. Benning, Physica B 205 (1995) 365.
[5] N.B. Brandt, V.V. Moshchalkov, Adv. Phys. 33 (1984) 373.
[6] D. Wohlleben, B. Wittershagen, Adv. Phys. 34 (1985) 403.
[7] P.C. Canfield, Z. Fisk, Phil. Mag. B 65 (1992) 1117.
[8] R.C. DeVries, J. Am. Ceram. Soc. 42 (1959) 547.
[9] M. Heinecke, K. Winzer, J. Noffke, H. Kranefeld, H. Grieb, K. Flachbart, Yu.B. Paderno, Z. Phys. B 98 (1995) 231.
[10] O. Gunnarsson, B.I. Lundqvist, Phys. Rev. B 13 (1976) 4274.
[11] A. Yanase, Fortran Program For Space Group, 1st Edition, Shokabo, Tokyo, 1995.